Histol Histopathol (2010) 25: 73-82

http://www.hh.um.es

Histology and Histopathology

Cellular and Molecular Biology

No loss of melanopsin-expressing ganglion cells detected during postnatal development of the mouse retina

Irene González-Menéndez, Felipe Contreras, Rafael Cernuda-Cernuda and José M. García-Fernández

Department of Morphology and Cell Biology, Oviedo University, Oviedo, Spain

Summary. Melanopsin, an opsin protein expressed in mammalian retinal ganglion cells (RGCs), makes them responsive to light. Such photosensitive RGCs form the retinohypothalamic tract (RHT) that provides signals to the suprachiasmatic nucleus (SCN), the master regulator of circadian rhythms. The SCN is adjusted daily to the environmental day/night cycle by signal inputs incoming from the RHT. In the present work we have studied, using immunohistochemistry techniques, the types and number of cells which expressed melanopsin during the postnatal development of pigmented C3H/He mice maintained in a standard daily cycle (12-h light / 12-h dark). Our results clearly show for the first time that the retina maintains a rather constant number of melanopsin-expressing RGCs from the first postnatal day and, thus, demonstrate that no loss of these photosensitive cells occurs during postnatal development. This supports the general idea that the non-image-forming system, in which these cells are involved, is functional at the very early postnatal stage.

Key words: Melanopsin, Postnatal development, Retina, Mice, Non-image-forming vision

Introduction

Retinal rods and cones are the primary photoreceptors for vertebrate image formation; however, sight is not the sole function of the retina. The so-called non-image forming vision, which basically consists of the perception of the day-night cycle and light intensity, is mediated by classical rod/cone photoreceptors and by a small subset of retinal ganglion cells (RGCs). Such RGCs express the photopigment melanopsin and are intrinsically photosensitive (ip) (Berson et al., 2002; Hattar et al., 2002). Such melanopsin-expressing cells also constitute the principal conduits for rod-cone input to non-image-forming vision (Güler et al., 2008) and project to several brain areas, including the suprachiasmatic nucleus (SCN), the organ in which the circadian rhythms that command the circadian physiology are generated (Gooley et al., 2001; Berson et al., 2002; Hannibal et al., 2002; Hattar et al., 2002; Panda et al., 2002; Ruby et al., 2002). In fact, it has been recently demonstrated that the targeted destruction of these ipRGCs alters the effects of light on circadian rhythms (Göz et al., 2008; Guler et al., 2008; Hatori et al., 2008). Some other major projections of these cells include the olivary pretectal nucleus, which controls pupil constriction and the intergeniculate leaflet, in which photic and non-photic circadian cues converge (Hattar et al., 2006). Minor innervation from the ipRGCs is also received in brain nuclei involved in the promotion of sleep, photic modulation of neuroendocrine outputs, image-forming vision, etc. (Hattar et al., 2006).

The different brain projections for image-forming and non-image-forming vision do not develop functionally at the same time. The onset of image-forming activity depends on the intraretinal synaptogenesis of cone/rod photoreceptors, the extraretinal ganglion cell synaptogenesis to the lateral geniculate nucleus and the eye opening, which occurs at postnatal day (P) 14 approximately (i. e., mice are totally image-blind until this postnatal day). However, the melanopsin-expressing ganglion cells are responsive to light stimulation since P0 (Sekaran et al., 2005; Tu et al., 2005). Moreover, it has been reported that the SCN begins to respond at P0-1 (Lupi et al., 2006), or at P4 (Muñoz-Llamosas et al., 2000) depending on light

Offprint requests to: José M. García-Fernández, Department of Morphology and Cell Biology, Oviedo University, 33071 Oviedo, Spain. e-mail: jmgf@uniovi.es

intensity. This means that functional connections between the retina and the SCN are already established at birth, when the production of RGCs is essentially complete (i.e. they all are postmitotic). A number of studies have described a neurotrophic cell death in the mouse ganglion cell layer (GCL) during the postnatal extraretinal and intraretinal synaptogenesis. A peak of RGC death occurs shortly after birth and a second peak seems to coincide with eye opening, approximately at the end of the second postnatal week (Valenciano et al., 2008). At least 70% of the RGCs generated are selected by programmed cell death during the three postnatal weeks (Strom and Williams, 1998).

Regarding the morphological and functional heterogeneity of ipRGCs in the mouse, previous works have identified two main cell types: M1 cells, with their dendritic arborisation in the outer-most sublayer of the inner plexiform layer (IPL), which corresponds to the sublamina a (OFF sublamina), and M2 cells, which have their dendrites forming a second plexus in the inner-most part of the IPL, which corresponds to the sublamina b (ON sublamina). Baver et al. (2008) demonstrated that these types have different brain projections, and in a recent study by Schmidt and Kofuji (2009) functional differences among them were also reported.

Although both the morphology and physiology of the melanopsin-expressing cells have been thoroughly analysed in mice, studies on their development are rather scarce to date (Sekaran et al., 2005; Tu et al., 2005; Lupi et al., 2006; Schmidt et al., 2008). Hence, our goal was to analyse the postnatal development of such photosensitive RGCs in pigmented C3H/He, mice in order to elucidate to what extent M1 and M2 cell subpopulations were affected by the selection occurring in the retina during the early postnatal period.

Materials and methods

Animals

Male and female pigmented mice *C3H/He* were used in the present study. Although commercially available *C3H/He* mice are retinally degenerate (*rd/rd*), we only studied C3H/He mice with normal retinas, i.e. wild-type at the *rd* locus (+/+), which were kindly donated by Dr. R. G. Foster (Oxford University, UK).

All the animals were maintained in the central animal care facilities under constant temperature conditions (20±2°C) and a 12-h light/12-h dark cycle, and fed with standard food and tap water ad libitum. Four ages were analysed: 1, 5, 11 and 21 postnatal (P) days, with a total of 4 animals per age group. The illumination source was a white light fluorescent lamp, so that the animals were exposed to a light intensity of 250±50 lux at cage level.

Tissue retrieval and preparation

In order to minimize pain, animals were anaesthetized prior to sacrifice. Animals were sacrificed 3 hours after light on. Experiments were performed in accordance with the European Communities Council Directive of 24 November 1986 (86/609/EEC).

Eyes from decapitated animals were removed and fixed in a 4% paraformaldehyde solution in 0.1M phosphate buffer (PB), pH 7.4, for 24 hours, and then washed in PB for 24 hours at 4°C.

Eye measurements

The diameter of the ocular globe, as well as the area of the whole flat-mounted retina, was measured at P1 and P21. Only one eye was analysed per animal. The diameter was measured by means of a gauge. The area of the photographed whole mount retinas was calculated with Corel Photopaint Software (Corel Corporation). The area was measured in pixels and then transformed in square millimetres.

Immunohistochemistry of retinal sections

For the immunohistochemistry techniques, the cornea and lens were removed. To obtain retinal sections the eyecup was dehydrated through a graded series of ethanol and embedded in paraffin. Sections of 10 µm were obtained from the paraffin blocks with a microtome (only one eye per animal was sectioned) and then mounted onto slides in six parallel series, of which only one was used for the present study. Paraffin sections were collected on gelatine-coated slides, deparaffined in xylene, hydrated in ethanol and placed in phosphate-buffered saline solution (PBS. 0,01M phosphate, 0,15M NaCl) for 10 min.

For the immunohistochemistry techniques, endogenous peroxidase activity was blocked by immersion in a solution of 0.3% hydrogen peroxide in PBS at room temperature (RT) for 30 minutes. Then they were washed twice for 5 minutes in PBS containing 0.4% Triton X-100 (PBS-T) at RT to enhance permeability. Unspecific binding was blocked with normal goat serum (Vector Labs) diluted in PBS for 30 min. at RT. This was followed by incubation with anti-melanopsin primary antibody (UF006, generously donated by Dr. Ignacio Provencio, University of Virginia, USA) at a dilution 1:5000 at 4°C for 3 days. Immunoreaction was visualized via the avidin-biotin-peroxidase method (Elite ABC kit, Vector Labs), using 0.025% DAB (3,-3'-diaminobenzidine tetrahydrochloride; Sigma) in 0.003% hydrogen peroxide Tris–HCl (0.05M, pH 7.5) buffer as chromogen. Finally, the sections were dehydrated in an ethanol series, cleared in eucalyptol, and coverslipped.

Immunofluorescence in flat mounted retinas

Flat-mounted retinas at P1 and P21 were also analysed. Four animals per age group and only one eye per animal were used. After eye fixation and washing,

the cornea and lens were removed and the retinas were isolated from the eyecup. Melanopsin immunohistochemistry was performed as described above, but with PBS-T containing 1% Triton X-100. Also, immunofluorescence with an Alexa-fluor 488 goat anti-rabbit antiserum (Invitrogen, with a dilution of 1:200), instead of the ABC method, was used. Finally, the retinas were mounted onto slides with mounting medium for fluorescence (Vectashield, Vector Labs), coverslipped and sealed.

Cell count and classification

The somata of melanopsin positive cells were counted, regardless of their localization or morphology, in the whole area of all the immunostained sections and of the flat-mounted retinas. For counting melanopsin positive cells on retinal sections a bright-field microscope was used (Nikon Eclipse E400). For whole flat-mounted retinas a confocal microscope was used (Leica TCS-SP2-AOBS). Melanopsin-positive cells were classified attending to the location of their soma and dendritic processes.

Statistical analysis

Student t test was used to compare ocular diameter and retinal area between P1 and P21. In total, the diameter of four eye globes and the area of four flat-mounted retinas were measured per age group.

A one-way ANOVA analysis was used to compare cell counts in retinal sections between ages P1, P5, P11 and P21. In flat mounted retinas Student t test was also used to compare total cell counts.

Results

The ocular globe diameter of pigmented mice increased significantly from P1 (2±0.04 mm) to P21 (3.025±0.05 mm) ($p<0.001$) (Fig. 1A,B). The retinal area also showed significant differences between P1 (5.25±0.30 mm^2) and P21 (14.03±0.39 mm^2) ($p<0.001$) (Fig. 1C,D), which means a 2.7-fold increase.

The UF006 antibody revealed immunoreactivity in somata, dendrites and proximal axonal segments of a RGC subpopulation. Melanopsin-expressing cells could be observed throughout the retina, at both the peripheral (Fig. 2A) and the central areas (Fig. 2B,C) from P1 on, and their somata were located either in the GCL or displaced in the INL. At P1 ipRGCs had already developed dendritic processes but they did not show any discrete plexus (Fig. 2D). At P11 we could observe two well-constituted plexuses in two sublayers of the inner plexiform layer (IPL): one plexus in the ON-sublayer (next to the GCL) and another in the OFF-sublayer (next to the INL). Dendritic processes in the ON plexus were finer and more numerous than those situated in the OFF plexus (Fig. 2E).

The total number of melanopsin-immunopositive cells in the retina did not vary significantly ($p>0.05$) during postnatal development. In retinal sections the number of melanopsin-positive cells ranged between 160 and 250 per retinal sample (P1, P5, P11, P21) (Fig. 3A). In whole flat-mounted retinas the number of melanopsin-positive cells ranged between 1600-1800 cells/retina (P1 to P21) (Fig. 3B). We have observed a similar total number of melanopsin-expressing cells in the retina at both ages. However, the total area of the retina increased during postnatal development (Fig. 4A,B) and, thus, the density of melanopsin-immunopositive cells decreased within the same period (Fig. 4C,D).

In the present study we have also analyzed and classified the melanopsin-expressing cells attending to the different location of their somata and dendritic processes from P5 on, since at P1 the different cell subtypes are not yet identifiable.

M1 cells

The dendritic processes of these cells were located in the outer margin of the IPL (OFF-sublayer). Two subtypes could be distinguished:

In the M1a cells the somata were located in the GCL and their dendritic processes were longer than those of M2 cells, showing prominent varicosities (Fig. 5A). These cells were frequently heavily stained, although some weakly stained cells with the same characteristics could also be detected.

M1b cells (approximately 10% of the total) had their somata displaced in the amacrine cells sublayer (i.e., the inner margin of the INL), and their dendrites were finer than those of M1a cells. Heavily (50%) (Fig. 5B) and weakly (50%) (Fig. 5C) stained cells with these characteristics could be observed.

M1 cells constituted about 22% of the total melanopsin-expressing cells during postnatal development and no differences between ages were detected. There was a roughly equal number of cells of subtypes 1a and 1b (Fig. 5D).

M2 cells

These cells had their dendritic processes in the inner margin of the IPL (ON side) and usually were weakly stained. Their bodies were located in the GCL (Fig. 6A). The percentage of M2 cells did not vary during postnatal development and ranged about 75% (Fig. 6B).

Some exceptions to this classification must be mentioned: a few immunostained cells, which constituted 0.5±0.1% of the total at all the ages studied had their bodies located in the amacrine cell layer and their processes in the inner margin of the IPL (ON sublayer) (not shown); moreover, we have observed some other cells that have their bodies located in the neuroblastic layer or in the INL and whose dendrites do

not branch into the IPL plexuses (not shown). A general decrease of these cell types during postnatal development was detected, so that at the end of this period their presence is merely occasional. Finally, the dendrites of a number of melanopsin-immunopositive cells seemed to arborize in the two plexuses of the IPL (not shown). All of these exceptions were not taken into account in the counts carried out for our study.

Discussion

Non-image forming vision is mediated by rod/cone photoreceptors and by melanopsin-expressing ipRGCs (Hattar et al., 2003; Panda et al., 2003). The latter

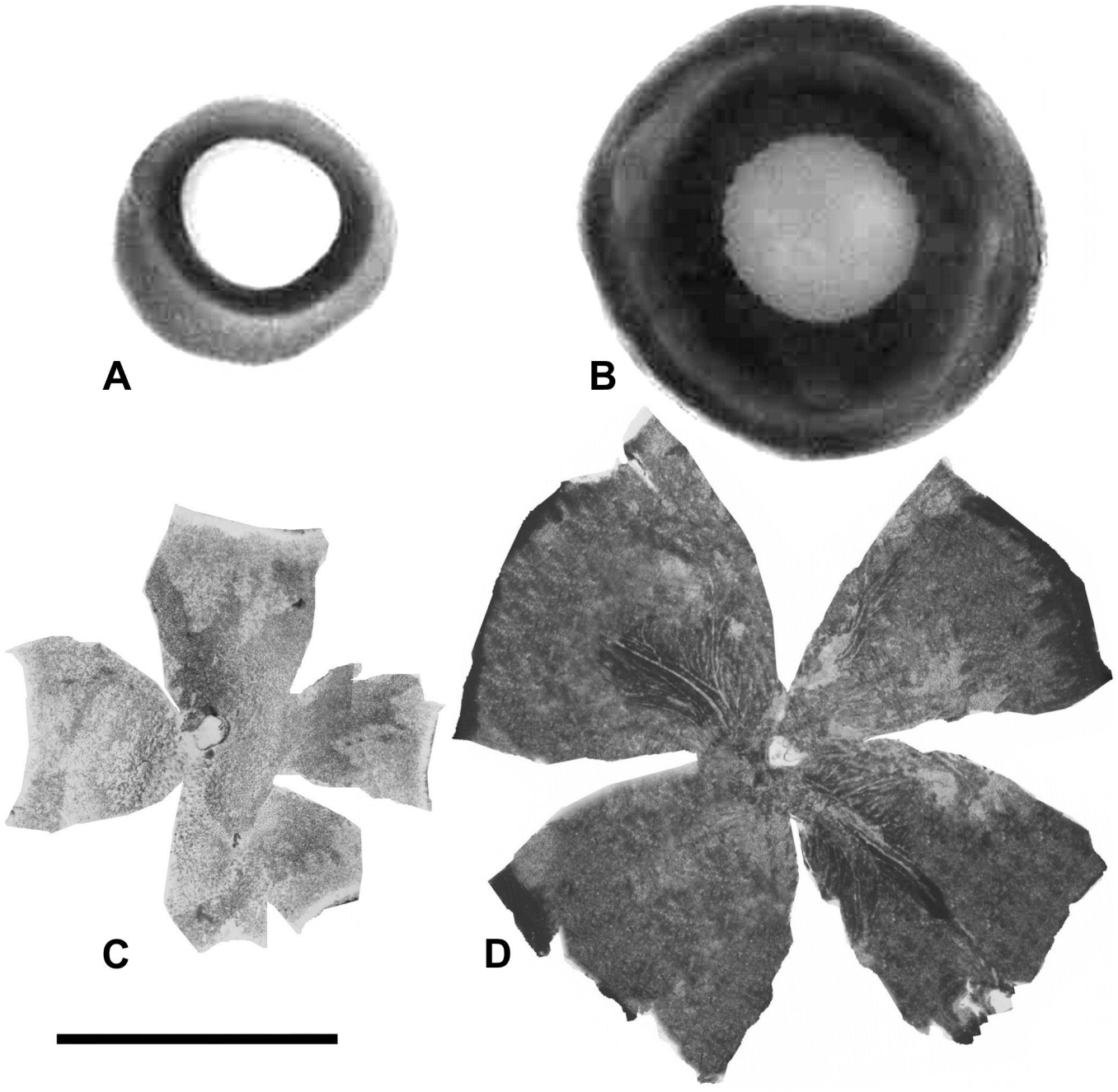

Fig. 1. C3H/He mice representative examples of ocular globes and flat-mounted retinas at P1 **(A, C)** and P21 **(B, D).** Note the increase in both the eye volume and the retinal area. Scale bar: 2 mm.

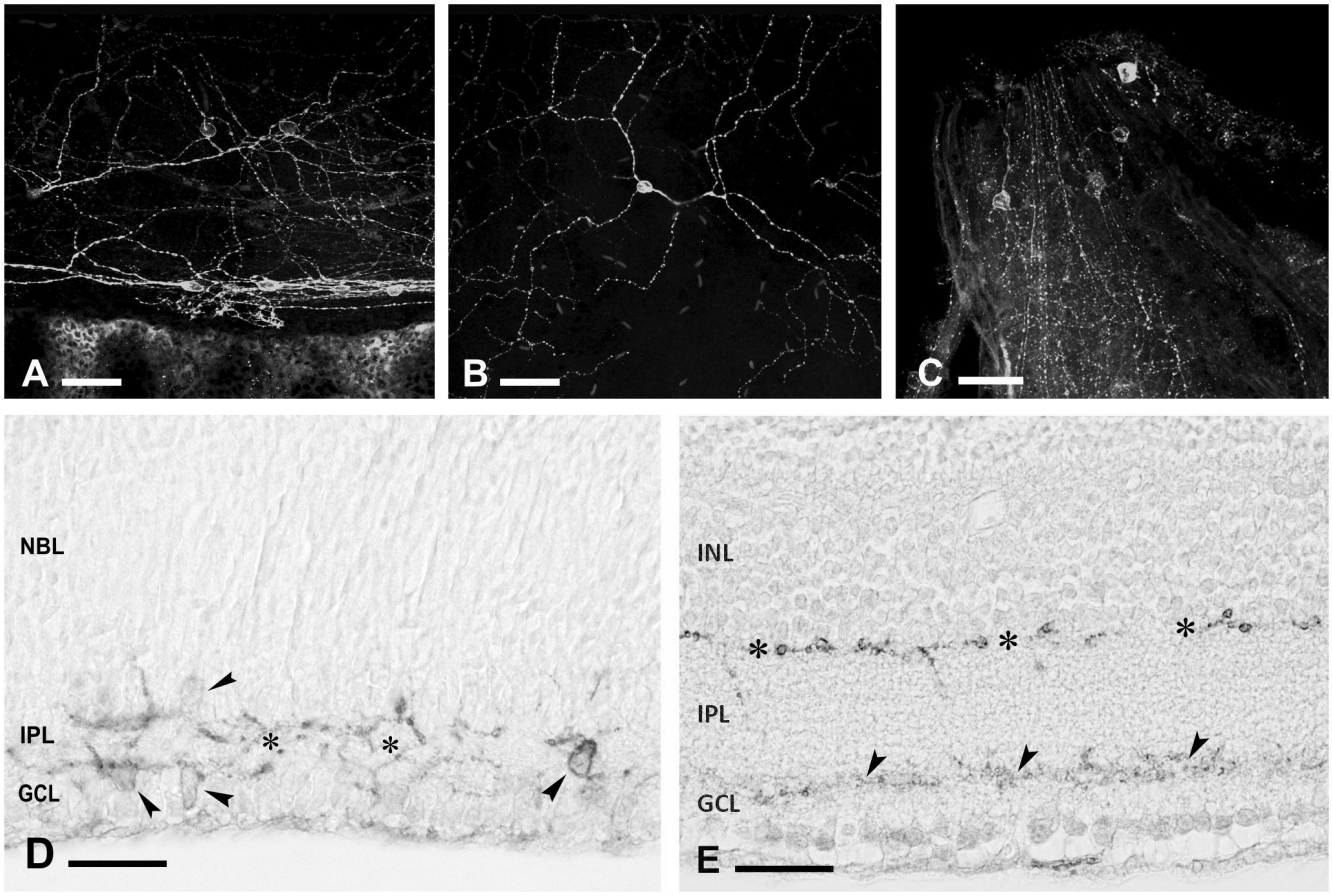

Fig. 2. Representative micrographs showing melanopsin-immunostained cells: with their somata located in the GCL, next to the ciliar body, and the dendrites situated in the inner plexus of the IPL **(A)**, with the soma situated in the INL, next to amacrine cells **(B)**, with the somata in the GCL near to the optic nerve **(C)**. Note that the axons also show immunoreactivity. Micrographs **A, B and C** correspond to whole-mounted retinas at P21. **D.** Retinal section with melanopsin-immunostained cells at P1: both the somata (arrowheads) and the dendrites (asterisks) can be recognised. **E.** The dendritic plexuses at P11 can be seen in the inner (arrowheads) and in the outer margin (asterisks) of the IPL in a retinal section. GCL: ganglion cell layer; IPL: inner plexiform layer; INL: inner nuclear layer; NBL: neuroblastic layer. Scale bars: 50 µm.

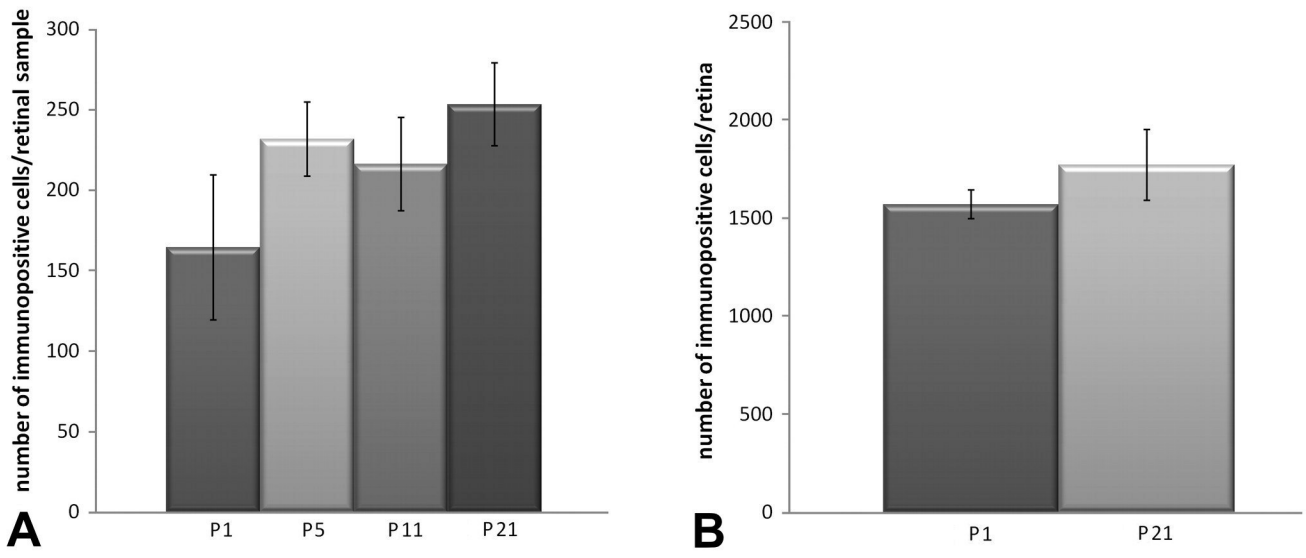

Fig. 3. A. Histogram showing the number of melanopsin-expressing cells per retinal sample (1 out of 6 series) (mean ± SEM) at the four postnatal ages analysed. No significant differences have been observed. **B.** Histogram showing the total number of melanopsin-expressing cells in whole-mounted retinas (mean ± SEM) at P1 and P21. No significant differences have been detected between these ages.

project to the suprachiasmatic nucleus, the master clock controlling circadian rhythms, and also to other brain nuclei involved in diverse functions, such as the promotion of sleep and pupil constriction, as well as some other aspects of image-forming vision (Hattar et al., 2006).

Melanopsin-expressing cells are responsive to light since the day of birth (Sekaran et al., 2005; Tu et al., 2005). During the development of the central nervous system a general overproduction of neuron cells occurs. The neurotrophic theory postulates that neuron survival is dependent on their successful competition for limited

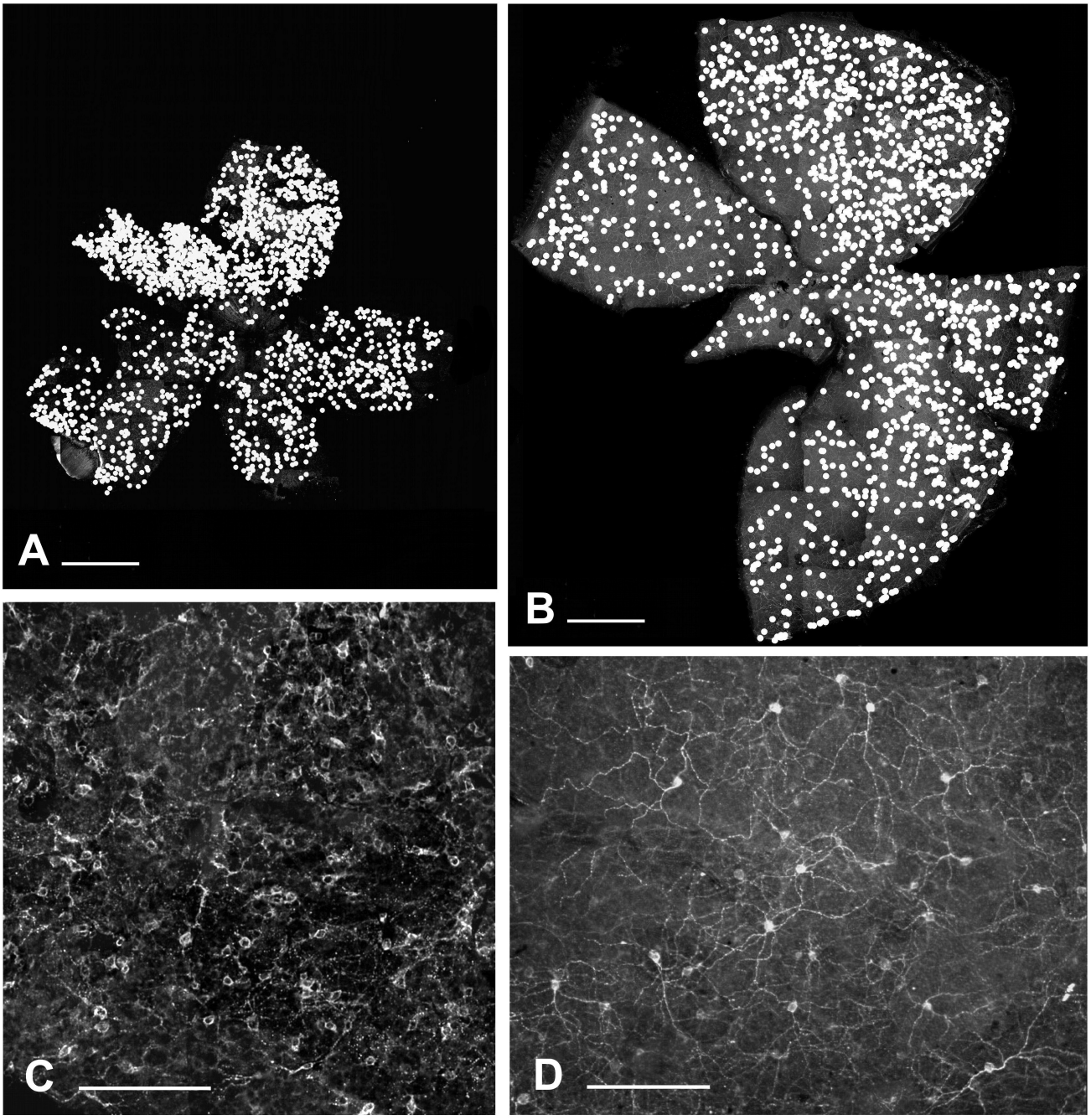

Fig. 4. Representative micrographs showing whole-mounted retinas at P1 **(A)** and P21 (**B**). Each white dot represents one melanopsin-expressing cell. Note also the difference in size of both retinas. Representative micrographs showing the cell densities at P1 **(C)** and at P21 **(D)**. Note that the cell density at P21 is lower than at P1. Scale bars: A, B, 750 µm; C, D, 150 µm.

neurotrophic factors secreted retrogradly by target cells. The ability of the neuron to compete for the survival factor will determine whether it survives or undergoes programmed cell death (apoptosis). In particular, many of the retinal neurons die from P2 to P15 (Valenciano et al., 2008). In C3H/He mice it has been described that 70% of RGCs die between P0 and adulthood (Strom and Williams, 1998). Regarding the melanopsin-expressing RGCs, little has been studied to date. Contrary to what some other authors found previously, our study provides evidence that no significant cell selection occurs after birth for the ipRGCs, a matter that is discussed below.

Sekaran et al. (2005) and Ruggiero et al. (2009) have reported a decrease in melanopsin immunopositive cells per mm^2 from the first postnatal days to adulthood. However, these authors do not seem to take into account that the retinal area increases considerably during postnatal development (a three-fold increase is reported in our results) and analyse their data as absolute values. Surprisingly, our results, which were obtained from

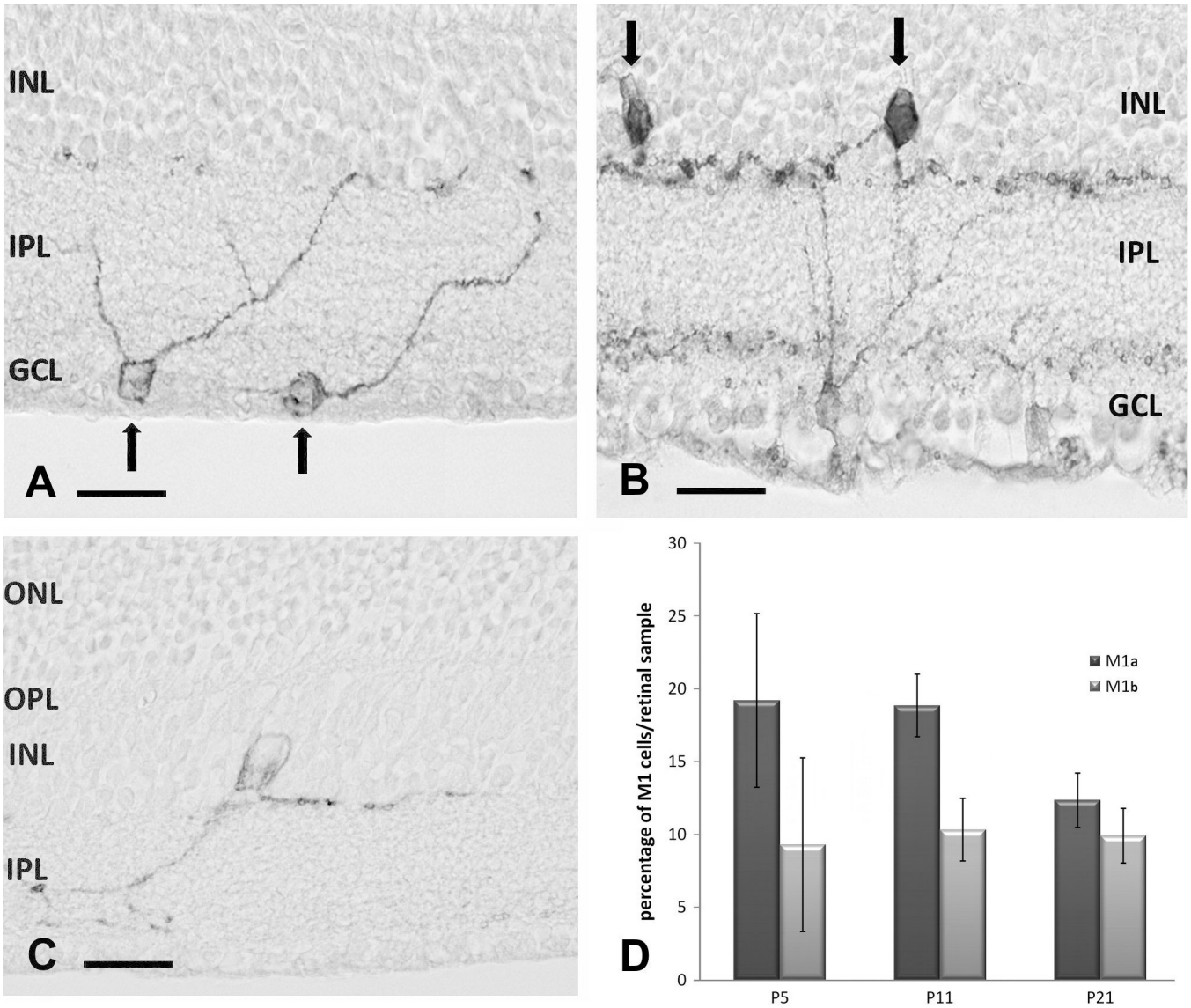

Fig. 5. Representative micrographs at PN21 showing some ipRGCs types. **A.** M1a cells have their somata located in the GCL and dendritic processes in the outer margin of the IPL (black arrow). **B.** M1b cells show heavily stained cell bodies located in the amacrine sublayer and dendritic processes in the outer margin of the IPL (black arrows). **C.** Weakly stained cell body located in the amacrine layer and dendritic processes in the outer margin of the IPL. **D.** Histogram showing the percentage of M1a and M1b melanopsin-expressing cells sampled in the retinal sections (mean ± SEM) at P5, P11 and P21. No significant differences between both cell subtypes have been detected during postnatal development. GCL: ganglion cell layer; IPL: inner plexiform layer; INL: inner nuclear layer; OPL: outer plexiform layer; ONL: outer nuclear layer. Scale bar: 50 µm.

retinal samples of the same mouse strain as that studied by Sekaran et al. and do refer to absolute values (immunopositive cells counted in one out of the six series obtained by sectioning the retinas completely and the total number of immunopositive cells when such cells were counted in the whole-mounted retinas), clearly show a rather constant number of melanopsin-expressing ganglion cells during postnatal development from P1 to P21 (160 to 250 immunostained cells/retinal sample, and 1600 to 1800 cells/retina). The three-fold increase of the total retinal area that we measured fits well with the three-fold decrease in cell density reported by Sekaran et al. (2005). The total number of melanopsin-expressing cells does not vary significantly from P1 to P21 and, therefore, a spatial reorganisation of these ipRGCs, rather than cell death, can be hypothesized for these cells during their postnatal development.

Sekaran et al. (2005) also detected a diminution in the density of light-responsive cells during postnatal development using Ca^{2+} imaging in the presence of carbenoloxone to block gap junctions and avoid correlated activity of neighboring non-ipRGCs. Such a decrease was particularly dramatic between P0 and P4. However, according to Tu et al. (2005), data obtained with this methodology during the first two postnatal days, P0 and P1, are not reliable, because in their experiments high doses of carbenoloxone could not prevent the activity of the neighboring cells within these postnatal days. Therefore, the decrease in ipRGCs between P0 and P4 observed by Sekaran et al. (2005) might be, at least in part, artifactual.

An important conclusion can be extracted from our finding: the melanopsin-expressing RGCs do not seem to experience significant apoptosis during the postnatal period. It is also known that melanopsin-expressing cells respond to light stimulation from P0 on (Sekaran et al., 2005). Moreover, the SCN responds to light since the very early postnatal period (Muñoz-Llamosas et al., 2000; Lupi et al., 2006), which means that functional connections between the retina and the SCN are established on the day of birth. We can thus infer that neurotrophic selection of melanopsin-expressing RGCs by programmed cell death, if it indeed occurs, might take place earlier than that of the remaining RGCs, which in principle are not involved in the non-image-forming vision. The latter begin to provide information to the central nervous system around P12, once the vertical synaptic connections between rod/cone photoreceptors and ganglion cells become functional (Sernagor et al., 2001).

We also analyzed ipRGCs morphology during postnatal development. In the mouse some ipRGCs have their dendritic processes branching in the sublamina a of the IPL (termed as M1 cells), while others do it in the sublamina b (termed as M2 cells). Different functional roles can be expected for these cells, since their dendritic arborisation is located either in the OFF area or in the ON area of the IPL, respectively (Schmidt and Kofuji, 2009). Some authors have even described a third type of ipRGCs whose dendrites branch in both sublayers (Viney et al., 2007; Schmidt et al., 2008). Although we occasionally found some of these cells, we preferred not to consider them in our analysis due to the difficulty to

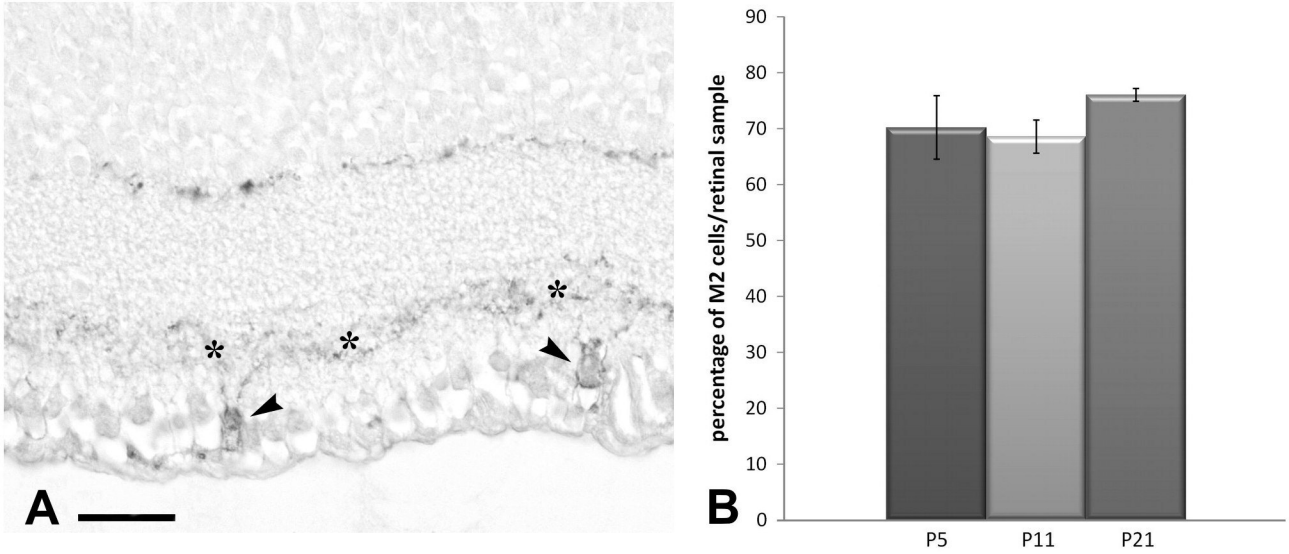

Fig. 6. A. M2 cells with their somata (arrowheads) located in the GCL and the dendritic processes in the inner margin of the IPL (asterisks). **B.** Histogram showing the percentage of M2 melanopsin-expressing cells sampled in the retinal sections (mean ± SEM) at P5, P11 and P21. No significant differences have been detected during postnatal development. GCL: ganglion cell layer; IPL: inner plexiform layer; INL: inner nuclear layer. Scale bar: 50 µm.

identify them, particularly in the retinal sections. We have observed the evolution of M1 and M2 cells, which showed stable percentages from P5 on. At P21 we detected 22% of M1 cells and 76% of M2 cells. Percentages of the cell types given in previous studies (Hattar et al., 2006; Baver et al., 2008) are difficult to fit with ours. The differences might be due to the use of different mice strains or techniques, or even to the time of the day in which the samples were collected, since the M1/M2 ratio was seen to vary within the 24-hour period (Gonzalez-Menendez et al., 2009). Moreover, we have observed differences in immunostaining intensity, which makes any comparative analysis even more complicated. Hattar et al. (2006), using the tau-lacZ marker gene to detect melanopsin-expressing cells, reported that B6/129 mice do not have ipRGCs that process in the inner margin of the IPL (i.e. M2 cells), hypothesizing that the melanopsin gene expression in these cells could be lower than in M1 cells. This might also be the explanation for the differences we observed in immunostaining intensity in our samples, i. e., the melanopsin expression in pale cells (weakly stained) could be lower than that of dark cells (heavily stained). As shown in our results, most of the M1 cells were dark and most of M2 cells were pale; however, exceptions occurred: for example, only half of the M1b cells (of those whose somata are located in the inner margin of the INL, constituting 10% of the total) were heavily stained. This would explain why Hattar et al. (2006) only detected 5% of immunopositive cells with their somata in the amacrine cell sublayer. Possibly, those showing low intensity of immunostaining in our samples were missed in their study.

In summary, the relevance of our study is to have reported that no apparent loss of ipRGCs occurs within the postnatal developmental period in the mouse. Moreover, the different cell types that express the photopigment melanopsin maintain their ratio from P5 on. These results support the general idea that the system these cells are involved in is functional at the very early postnatal stage. We think this work contributes to a better understanding of the development of the non-image-forming visual system. Further research must be carried out in order to find out the differential roles of the ipRGCs types in both the image-forming and non-image-forming visual systems, as well as their potential involvement in the control of the retinal clock.

Acknowledgements. The UF006 antiserum was generously donated by Dr. Ignacio Provencio, University of Virginia, USA. The C3H/He mice (Wild-type at the rd locus) were kindly donated by Dr. Russell G. Foster (Oxford University, UK). This study was supported by Grant BFU2006-15576 (from the Spanish Ministry of Science and Innovation) to J.M. G.-F. I. G.-M was supported by fellowship BP07-088 (from the Spanish FICYT).

References

Baver S.B., Pickard G.E., Sollars P.J. and Pickard G.E. (2008). Two types of melanopsin retinal ganglion cell differentially innervate the hypothalamic suprachiasmatic nucleus and the olivary pretectal nucleus. Eur. J. Neurosci. 27, 1763-1770.

Berson D.M., Dunn F.A. and Takao M. (2002). Phototransduction by retinal ganglion cells that set the circadian clock. Science 295, 1070-1073.

Gonzalez-Menendez I., Contreras F., Cernuda-Cernuda R. and Garcia-Fernandez J.M. (2009). Daily rhythm of melanopsin-expressing cells in the mouse retina. Front. Cell. Neurosci. 3:3. doi: 10.3389/neuro.

Gooley J.J., Lu J., Chou T.C., Scammell T.E. and Saper C.B. (2001). Melanopsin in cells of origin of the retinohypothalamic tract. Nat. Neurosci. 12, 1165.

Göz D., Studholme K., Lappi D.A., Rollag M.D., Provencio I. and Morin L.P. (2008). Targeted destruction of photosensitive retinal ganglion cells with a saporin conjugate alters the effects of light on mouse circadian rhythms. PLoS ONE 3, e3153.

Güler A.D., Ecker J.L., Lall G.S., Haq S., Altimus C.M., Liao H.W., Barnard A.R., Cahill H., Badea T.C., Zhao H., Hankins M.W., Berson D.M., Lucas R.J., Yau K.W. and Hattar S. (2008). Melanopsin cells are the principal conduits for rod-cone input to non-image-forming vision. Nature 453, 102-105.

Hannibal J., Hindersson P., Knudsen S.M., Georg B. and Fahrenkrug J. (2002). The photopigment melanopsin is exclusively present in pituitary adenylate cyclase-activating polypeptide-containing retinal ganglion cells of the retinohypothalamic tract. J. Neurosci. 22, 191-197.

Hatori M., Le H., Vollmers C., Keding S.R., Tanaka N., Buch T., Waisman A., Schmedt C., Jegla T. and Panda S. (2008). Inducible ablation of melanopsin-expressing retinal ganglion cells reveals their central role in non-image forming visual responses. PLoS ONE 3, e2451.

Hattar S., Liao H.W., Takao M., Berson D.M. and Yau K.W. (2002). Melanopsin-containing retinal ganglion cells. Science 295, 1065-1075.

Hattar S., Lucas R.J., Mrosovsky N., Thompson S., Douglas R.H., Hankins M.W., Lem J., Biel M., Hofmann F., Foster R.G. and Yau K.W. (2003). Melanopsin and rod-cone photoreceptive systems account for all major accessory visual functions in mice. Nature 424, 76-81.

Hattar S., Kumar M., Park A., Tong P., Tung J., Yau K.W. and Berson D.M. (2006). Central projections of melanopsin-expressing retinal ganglion cells in the mouse. J. Comp. Neurol. 497, 326-349.

Lupi D., Sekaran S., Jones S.L., Hankins M.W. and Foster R.G. (2006). Light-evoked FOS induction within the suprachiasmatic nuclei (SCN) of melanopsin knockout (Opn4-/-) mice: a developmental study. Chronobiol. Int. 23, 167-179.

Muñoz-Llamosas M., Huerta J.J., Cernuda-Cernuda R. and García-Fernández J.M. (2000). Ontogeny of a photic response in the retina and suprachiasmatic nucleus in the mouse. Brain Res. Dev. Brain Res. 15, 1-6.

Panda S., Sato T.K., Castrucci A.M., Rollag M.D., DeGrip W.J., Hogenesch J.B., Provencio I. and Kay S.A. (2002). Melanopsin (Opn4) requirement for normal light-induced circadian phase shifting. Science 298, 2213-2216.

Panda S., Provencio I., Tu D.C., Pires S.S., Rollag M.D., Castrucci A.M., Pletcher M.T., Sato T.K., Wiltshire T., Andahazy M., Kay S.A., Van Gelder R.N. and Hogenesch J.B. (2003). Melanopsin is required for non-image-forming photic responses in blind mice. Science 301, 525-527.

Ruby N.F., Brennan T.J., Xie X., Cao V., Franken P., Heller H.C. and O'Hara B.F. (2002). Role of melanopsin in circadian responses to light. Science 298, 2211-2213.

Ruggiero L. Allen C.N., Brown R.L. and Robinson D.W. (2009). The development of melanopsin-containing retinal ganglion cells in mice with early retinal degeneration. Eur. J. Neurosci. 29, 359-367.

Schmidt T.M. and Kofuji P. (2009). Functional and morphological differences among intrinsically photosensitive retinal ganglion cells. J. Neurosci. 29, 476-482.

Schmidt T.M., Taniguchi K. and Kofuji P. (2008). Intrinsic and extrinsic light responses in melanopsin-expressing ganglion cells during mouse development. J. Neurophysiol. 100, 371-84.

Sekaran S., Lupi D., Jones S.L., Sheely C.J., Hattar S., Yau K.W., Lucas R.J., Foster R.G. and Hankins M.W. (2005). Melanopsin-dependent photoreception provides earliest light detection in the mammalian retina. Curr. Biol. 15, 1099-1107.

Sernagor E., Eglen S.J. and Wong R.O. (2001). Development of retinal ganglion cell structure and function. Prog. Retin. Eye. Res. 20, 139-174.

Strom R.C. and Williams R.W. (1998). Cell production and cell death in the generation of variation in neuron number. J. Neurosci. 18, 9948-9953.

Tu D.C., Zhang D., Demas J., Slutsky E.B., Provencio I., Holy T.E. and Van Gelder R.N. (2005). Physiologic diversity and development of intrinsically photosensitive retinal ganglion cells. Neuron 48, 987-999.

Valenciano A.I., Boya P. and de la Rosa E.J. (2008). Early neural cell death: numbers and cues from the developing neuroretina. Int. J. Dev. Biol. 52. doi: 10.1387/ijdb.072446av.

Viney T.J., Balint K., Hillier D., Siegert S., Boldogkoi Z., Enquist L.W., Meister M., Cepko C.L. and Roska B. (2007). Local retinal circuits of melanopsin-containing ganglion cells identified by transsynaptic viral tracing. Curr. Biol. 17, 981-988.

Accepted August 27, 2009